THE JOURNAL OF PHYSICAL CHEMISTRY B

Article

pubs.acs.org/JPCB

Effect of Hydration on Structural and Thermodynamic Properties of Pig Gastric and Bovine Submaxillary Gland Mucins

Yana Znamenskaya,* Javier Sotres, Johan Engblom, Thomas Arnebrant, and Vitaly Kocherbitov

Biomedical Science, Faculty of Health and Society, Malmö University, SE-205 06 Malmö, Sweden

Supporting Information

ABSTRACT: One of the essential functions of mucous gel is protection of tissues against dehydration. The effect of hydration on the structural and thermodynamic properties of pig gastric mucin (PGM) and bovine submaxillary gland mucin (BSM) have been studied using atomic force microscopy (AFM), sorption, and differential scanning calorimetry (DSC). The analysis of sorption isotherms shows the higher water sorption capacity of PGM compared to BSM at RH levels lower than about 78%. The value of the hydration enthalpy at zero water content at 25 °C for both biopolymers is about −20 kJ/mol. Glass transitions of BSM and PGM occur at RH levels between 60 and 70% for both mucins. AFM indicates the presence of a dumbbell structure as well as a fiber-like structure in PGM samples. The experimental volume of the dry dumbbell molecule obtained by AFM is 3140 ± 340 nm^3. Using DSC data, the amount of nonfreezing water was calculated to be about 0.51 g/g of PGM. The phase diagram of PGM demonstrates two regions of different Tg: dependent and independent of hydration levels. In particular, at mucin concentrations from 0 to 67 wt %, the glass transition occurs at a constant temperature of about −15 °C. At higher concentrations of mucin, Tg is increasing with increasing mucin concentrations.

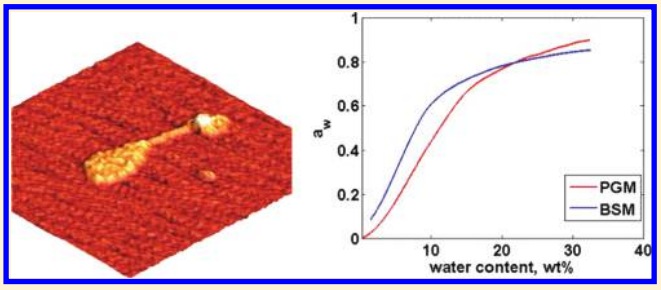

INTRODUCTION

Mucous secretions play an important role in animal and human life.[1,2] The mucous barrier and its transport properties are essential for proper functioning of the digestive, respiratory, and reproductive systems of vertebrates, including humans.[3,4] The most important biological functions of mucus are maintenance of a hydrated layer covering the epithelium, a barrier to pathogens and noxious substances, the first barrier with which nutrients and delivered drugs will interact.[5] From an engineering point of view, mucus is an outstanding water-based lubricant.[3] One of the essential functions of the mucous gel is protection of tissues against dehydration (drying). In order to fulfill this function, the mucous gel should be strongly hydrated; i.e., it should contain a large amount of water. The presence of a large amount of water prevents strong changes of water activity in the mucous gel when the relative humidity (RH) of the surrounding atmosphere changes. Nonetheless, when subjected to a long contact with dry atmosphere, mucous gel dries out. Usually mucous secretions contain 95% water.[3,5] For example, "in vitro", at a typical value of 30% RH (in equilibrium with atmosphere), the mucus contains approximately 10 vol % of water,[6] which means it is dehydrated. "In vivo", below 30% RH, the eyes and skin become dry, and below 10% RH, the nasal mucous membrane becomes dry as well as skin and eyes.[7] Consequently, dehydration of mucous gel changes its protective properties and may become a pathogenic factor in many diseases[1] such as cystic fibrosis,[2,8,9] asthma,[2] gastric carcinoma,[10] primary Sjogren's syndrome (PSS),[11] and rhinorrhea.[12] These examples show that hydration "in vivo" as well as "in vitro" play an important role in the biological processes and attract significant attention in science.

Mucus consists primarily of water (~95%), glycoprotein mucin, and other molecules—enzymes, proteins, electrolytes, and lipids[5,13−16]—the concentration of which depends on the mucus source. The principal component of mucus, forming its macromolecular matrix and dominating its rheological properties, is mucin.[13,14,17] Mucins are large glycoproteins with high molecular weight ranging from 0.5 to 40 MDa.[5,18] They are expressed in epithelial and glandular tissues.[19] Mucins have been given a gene symbol MUC, followed by a number.[2] At the present moment, nearly 20 MUC genes have been found but not all are fully sequenced.[2,4,5,20] Mucin molecules are highly glycosylated.[5,18] The carbohydrate content can be up to 80% of the total mass of the molecule, and consists of *N*-acetylgalactosamine, *N*-acetylglucosamine, fucose, galactose, and sialic acid.[21] The carbohydrates are present as short chains, often branched, and attached to the polypeptide chain by O-glycosidic bonds to the −OH group of serine and threonine residues.[21] The size of the carbohydrate side chains depends on the origin of mucous secretion and varies from 2 and 5 sugars per chain (sheep and pig submaxillary mucus) up to 16 or 19 sugars per chain (human ovarian cyst and pig gastric mucus).[1] All mucin polypeptide chains have domains rich in threonine and/or serine whose hydroxyl groups are in O-glycosidic linkage with

Received: December 27, 2011
Revised: March 28, 2012
Published: March 28, 2012

oligosaccharides.[4] Moreover, these domains are composed of tandemly repeated sequences that vary in number, length, and amino acid sequence from one mucin to another.[22] Due to the large molecular weight of mucin, its polydispersity, and its high degree of glycosylation,[5] it has been difficult to characterize mucin structure. Mucin molecules can be described by different models.[1,3,16,23−25] Often it is described as a bottle-brush model: a copolymer of relatively rigid (glycosylated) and relatively flexible (naked) moeties.[1,3,16,23] However, pig gastric mucin has also been described as a dumbbell pattern, presented as two symmetric globules per chain separated by a heavily glycosylated spacer[25] or as two asymmetric globules separated by a hydrophilic part which is glycosylated.[24]

The exact phase behavior of mucin as a function of temperature and hydration levels has yet to be determined. The phase behavior of mucins has been studied by several authors using different techniques.[3,16,26−28] Viney et al.[27] studied slug pedal mucin by cross polarized light microscopy and suggested that it forms nematic liquid crystals. Later, Viney[28] investigated the formation of liquid crystalline domains in partially dried giraffe saliva by polarized light microscopy. Waigh et al.[29] studied pig gastric mucin using light scattering measurements, small angle neutron scattering (SANS), and rheological experiments. They observed a polydomain nematic phase in porcine stomach mucin at concentrations above 21 mg/mL and suggested four regimes for the mucin phase behavior as a function of concentration. The phase behavior of commercially available pig gastric mucin as a function of temperature and concentration has been studied by Davies and Viney.[3] Using differential scanning calorimetry (DSC) and polarized light microscopy, these authors presented a partial phase diagram for the water/mucin system, where the glass transition is independent of concentration and occurs at 24.8 °C. Results obtained by Momoh et al.[26] indicated glass transition at 111 °C in snail mucin by DSC study. Builders et al. presented the onset and the end of the glass transition of porcine mucin at 40.4 and 68.6 °C, respectively, using the DSC method.[30] These data suggest that the temperatures of glass transition may be different for different types of mucins. Another source of discrepancies between glass transition temperatures in the works cited above can be in differences in experimental conditions, especially water contents. In this work, we will show that the glass transition temperature of mucin is strongly dependent on water content.

It is known from the literature that water sorption isotherms of pedal mucus trails,[6] porcine mucin,[30] and bovine and porcine submaxillary mucins[31] have been presented using gravimetric methods. Here we present sorption isotherms of PGM and BSM obtained with sorption calorimetry. As far as we know, water/mucin systems have never been studied using the sorption calorimetric method. Previous sorption calorimetric studies demonstrate that the method is useful for studies of the hydration of proteins, polymers, and surfactants.[32−36] This method allows simultaneous measurements of the water activity a_w and the partial molar enthalpy of mixing of water H_w^{mix}.[37] In this work, the glass transition, the sorption isotherms, and the partial molar enthalpy of mixing of water of pig gastric and bovine submaxillary mucins have been measured using sorption calorimetry. In addition, the method of atomic force microscopy (AFM) was used to characterize the structure of both types of mucin molecules when deposited on the mica surface, which indicate the dumbbell structure of PGM. Also, using differential calorimetric data, the amount of protein-bound water was calculated. The phase diagram of PGM was constructed using the data from sorption and differential scanning calorimetry.

MATERIALS AND METHODS

Mucin. In this study, samples from porcine gastric mucin (PGM), mucin from bovine submaxillary glands (BSM), and dried mucus from a slaughtered pig (crude PGM, PGMC) were used.

Commercially available, partially purified PGM type III, containing 0.5−1.5% bound sialic acid (Sigma, USA; cat. no. M1778, lot no. 018K7001) and BSM (cat. no. M3895, lot no. 016K7001), type I−S, containing 9−17% bound sialic acids were purchased from Sigma.

Mucosa from a slaughtered pig's stomach (PGMC) was gently scraped off with a scalpel and immersed in a plastic test tube which was stored in a freezer at −80 °C before experiments. Mucosa contains a large amount of water (∼95%), so first it was dehydrated in freeze-dryer for 72 h. Then, the drying process continued in a vacuum at room temperature in contact with 3 Å molecular sieves for 48 h to complete dehydration. Calculation of masses before and after drying indicated that PGMC contains 95% water and 5% solids.

Ultrahigh quality (UHQ) water, purified at 25 °C by Elgastat UHQ II Model UHQ-PS-MK3 (Elga Ltd., High Wycombe, Bucks, UK), was used as a solvent. To prevent microorganism growth, UHQ water contained 0.1 wt % sodium azide (Kebolab, USA, cat. no. UN1687).

For AFM experiments, stock PGM and BSM solutions (1 wt % mucin) were diluted to concentrations of 10^{-3}, 10^{-5}, and 10^{-6} wt % mucin that allowed visualization of individual structures. A 50 μL portion of diluted mucin solution was pipetted onto a freshly cleaved mica substrate (Electron Microscopy Sciences, Fort Washington, PA) and allowed to dry in a laminar-flow chamber to prevent contamination of the surface. Samples were analyzed in the AFM immediately after drying.

In the sorption calorimetric measurements, completely dry samples are required, i.e., the initial water activity in samples should be zero. BSM, PGM, and PGMC were dried in a vacuum at room temperature in contact with 3 Å molecular sieves for 24−48 h directly prior to the experiments. To compare the accuracy of sorption calorimetric experiments, dry PGM samples were equilibrated in desiccators with saturated salt solutions at 25 °C. The PGM−water mixtures were weighed to obtain the sorption isotherm. The following salts were used: KNO_3, $Mg(NO_3)_2$, NaCl, $MgCl_2$, CH_3COOK, and LiCl.

For differential scanning calorimetry, samples with different mucin concentrations (wt %) were prepared by adding the appropriate amount of solvent to a weighed amount of dry PGM. After mixing mucin with water, samples were left for equilibration for several days. To avoid errors in concentration of the mixtures, PGM was completely dried in a vacuum at room temperature before adding solvent to the dry glycoprotein. Mixtures with concentrations above 50 wt % PGM were not homogeneous after equilibration. Therefore, mixtures with low water contents were prepared using another method. Completely dry PGM was equilibrated in desiccators with saturated salt solutions which give different relative humidity levels[38] for 7−10 days at 25 °C. Water vapor was absorbed by dry mucin, the PGM−water mixtures were weighed to obtain the water content, and then samples were

dx.doi.org/10.1021/jp212495t | J. Phys. Chem. B 2012, 116, 5047−5055

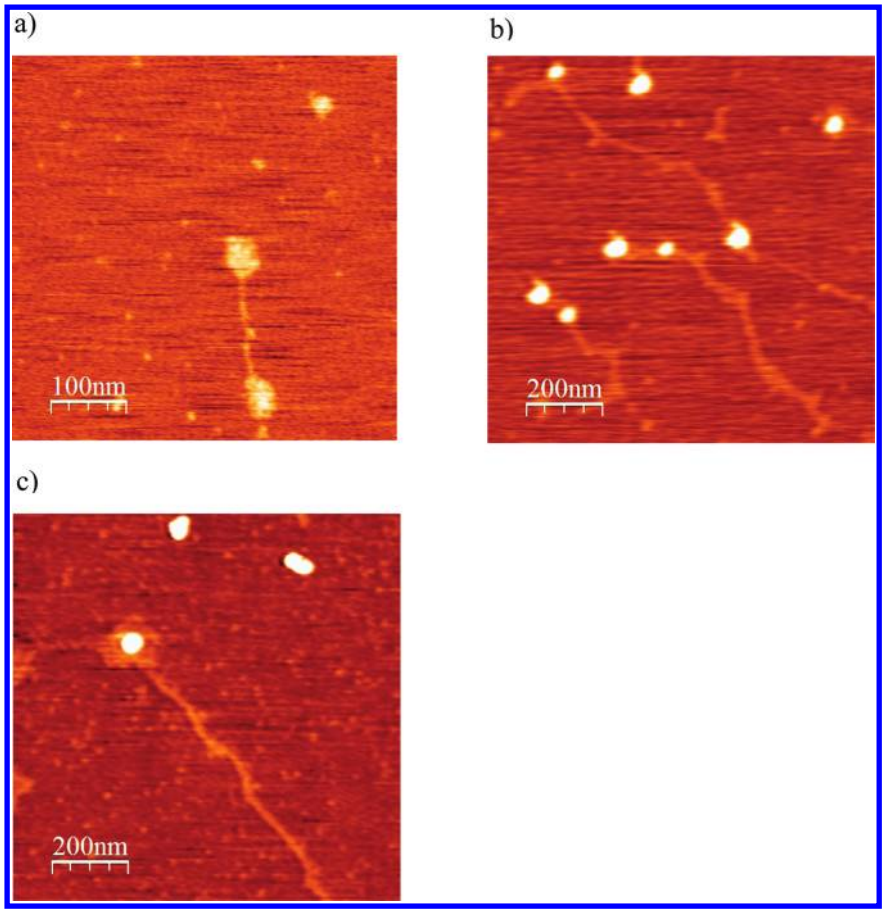

Figure 1. AFM images of the evaporated mucin drop on mica: (a) PGM dumbbell-like structure (concentration during adsorption = 10^{-5} wt %); (b) PGM fiber-like structure (concentration during adsorption = 10^{-3} wt %); (c) BSM fiber-like structure (concentration during adsorption = 10^{-5} wt %).

examined by DSC. The following salts were used: KNO_3, $Mg(NO_3)_2$, NaCl, $MgCl_2$, and CH_3COOK.

AFM. Atomic force microscopy (AFM) images were obtained using a commercial setup (Multimode SPM with a Nanoscope IV control unit, Veeco Instruments, Santa Barbara, CA). The AFM was operated in tapping mode, where the cantilever is oscillated at its free resonance frequency, and the tip−sample distance adjusted while scanning so that the amplitude of the oscillation is kept constant. All images were obtained in air at room temperature. Silicon cantilevers with a nominal resonance frequency between 320 and 364 kHz were used in all of the experiments (RTESP7; Veeco Probes, Camarillo, CA).

Analysis and processing of AFM images was performed with the WSxM software.[39] Standard image processing consisted of plane subtraction and/or equalization.

Sorption Calorimetry. The sorption calorimetric method was used to study the hydration of glycoprotein mucin. This method allows one to simultaneously measure the water activity a_w and the partial molar enthalpy of mixing of water H_w^{mix}.[37] The sorption calorimetric experiments were performed at 25, 40, and 50 °C in a 28 mm two-chamber calorimetric cell inserted in a double-twin microcalorimeter.[40] The dry sample is placed in the upper (sorption) chamber, and pure water is injected in the lower (vaporization) chamber. Evaporated water diffuses through the tube which connects the upper and lower chambers of the calorimetric cell and is absorbed by dry sample. The activity of water is calculated from the thermal power of evaporated water registered in the vaporization chamber.[41] The partial molar enthalpy of the mixing of water is calculated using the following equation:

$$H_w^{mix} = H_w^{vap} + H_w^{vap}\frac{P^{sorp}}{P^{vap}} \quad (1)$$

where P^{vap} and P^{sorp} are the thermal powers registered in the vaporization and sorption chambers, respectively, and H_w^{vap} is the molar enthalpy of evaporation of pure water.[37]

Differential Scanning Calorimetry (DSC). Mucin samples at different hydration levels were examined using a differential scanning calorimeter (DSC 1 Mettler Toledo). The samples were cooled down to −80 °C, held 10 min at this temperature, and then heated to 95 °C with a scan rate of 5 °C/min. In addition, to compare to results obtained by Davies and Viney, our PGM samples were examined at the same conditions as in their study of mucin.[3] Calibration for heat flow and temperature was done using indium (mp 156.6 °C; ΔH = 28.45 J/g). Samples were inserted into a 40 μL aluminum pan, hermetically sealed, and studied immediately after preparation. An empty sealed pan was used as a reference during all experiments. The furnace chamber was purged with a dry nitrogen gas flowing at 80 mL/min.

RESULTS AND DISCUSSION

AFM. To characterize the molecular structure of PGM and BSM, solid residues from evaporated mucin solutions on mica were visualized in air at room temperature by atomic force

dx.doi.org/10.1021/jp212495t | J. Phys. Chem. B 2012, 116, 5047−5055

microscopy (AFM). We performed imaging of dried samples, as, in this case, all the material present in the mucin solution will be eventually deposited in the mica surface and, therefore, visualized. This is in contraposition to imaging in liquid, where only the material strongly adsorbed on the surface would have been visualized. AFM measurements of PGM indicated both dumbbell-like (Figure 1a) and fiber-like (Figure 1b) structures. The globule height is about 1 nm, and the height of the spacer which separates globules is 0.5 nm (Figure 1a). The height of the fiber-like structures (Figure 1b) is about 1 nm, and they could extend from a few tens of nanometres up to more than a micrometer. Parts b and c of Figure 1 show also globules with heights from 7 to 11 nm, which can be assumed to be mucin aggregates. The heights measured for both dumbbell-like and fiber-like structures are smaller than the PGM molecule sizes reported in the literature.[24,25] It can be explained by the effect of sample preparation. During the dehydration, the PGM molecules become flatter on the mica surface. As a result, the obtained heights of the molecules are smaller than the original size of the mucin. The dumbbell-like structures showed a high dispersion in their horizontal dimensions, usually with asymmetric globules separated by distances that could go from 20 nm up to almost 150 nm. However, volume calculations yielded similar values for all the visualized dry dumbbell-like structures, with an average value of 3140 ± 340 nm^3. The relatively small dispersion obtained for the calculated volumes can be considered as an indicator of the visualized dumbbell-like structures corresponding to the same molecule. The volume of dry PGM molecules obtained in AFM can be compared to the volume of the globule in dumbbell structure in bulk solution calculated by the equation $V = 4/3\pi R^3$, where R is the average radius of the globule, ~10 nm.[24,25] Thus, the calculated volume of the sphere is about 4189 nm^3, so the volume for two globules per chain is 8378 nm^3. Also, the volume can be calculated, using the molecular weight of the mucin molecule ($M_w \sim 546$ kDa[25] and $\rho \sim 1200$ kg/m^3), and it is equal to 1511 nm^3 for the dumbbell-like mucin structure. The value of the dry experimental volume is between calculated values using literature data, and has the same magnitude, which supports the results obtained in AFM.

For BSM samples, only fiber-like structures were observed (Figure 1c). The height of fibers in BSM is similar to those which have been indicated for PGM, and it is about 1 nm.

As it follows from the literature, mucin molecules obtained from different sources have different structures that can be described by models ranging from the bottle brush[1,3,16,23] to dumbbell type.[24,25] For example, fiber-like structures of PGM[42,43] and ocular[44] mucin as well as the globular structure of human cervical mucus[45] and PGM[46] have been obtained by AFM. Thus, the different models of PGM molecules can be explained by the presence of several mucins in the stomach mucus layer.[47−50] The cells in the surface epithelium of pig gastric mucosa produce different mucins. For instance, Nordman et al.[48,50] have shown gastric mucosa containing both MUC5AC and MUC6 mucins. Reis et al.[49] described stomach with MUC1, MUC2, MUC5AC, and MUC6 mucins. And often mucins from the pig gastric mucosa are described as the bottle brush model.[1,3,16,23] However, the daisy chain configuration of pig gastric mucin, MUC6, has been described by Di Cola et al.[24] and Yakubov et al.[25] Consequently, as expected for pig PGM molecules, different structures were obtained by AFM. Figure 1a,b shows the presence of a dumbbell structure as well as a fiber-like structure in PGM samples.

Sorption Calorimetry. Sorption calorimetric experiments on PGM and BSM were done at 25, 40, and 50 °C. As an example, the water sorption isotherm of PGM at 25 °C is presented in Figure 2. In addition to sorption calorimetry, the

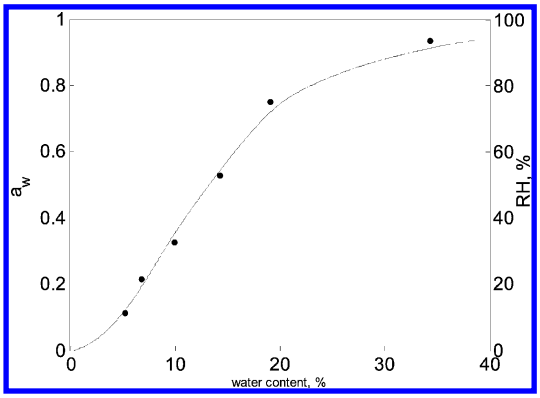

Figure 2. Water activity of PGM as a function of water content at 25 °C: solid line, data from sorption calorimetry; ●, data from experiment with saturated salt solutions: KNO_3, NaCl, $Mg(NO_3)_2$, $MgCl_2$, CH_3COOK, LiCl. Humidity level is calculated using the following equation: RH = a_w·100%.

method with saturated salt solutions was used to obtain the sorption isotherm of PGM. Mucin samples were equilibrated at 25 °C with water vapor from saturated salt solutions which give the known relative humidity level.[38] Results are shown together with sorption calorimetric data in Figure 2. It demonstrates a good agreement of sorption isotherms of PGM obtained by two different methods.

Figure 3 shows the water activity in the hydrated mucin systems at 25, 40, and 50 °C. Sorption isotherms both of PGM (Figure 3a) and BSM (Figure 3b) demonstrate an increase of water activity with increasing temperature at low water contents. An explanation can be given by using data of the enthalpy of mixing water for PGM and BSM (Figure 4) and the following equation:[33]

$$\frac{\mathrm{d} \ln a_w}{\mathrm{d}T} = -\frac{H_w^m}{RT^2} \quad (2)$$

According to eq 2, an increase of the water activity in mucin mixtures with increasing temperature at low water content is promoted by negative values of the partial molar enthalpy of mixing of water, H_w^m. As the enthalpy of hydration at high water content is close to zero, that leads to a weaker dependence of water activity on temperature.[33]

Sorption isotherms between BSM and PGM have been compared at 25, 40, and 50 °C. For instance, results for 40 °C are shown in Figure 5. The sorption isotherm of PGM shows higher water sorption capacity at RH levels lower than 77%. BSM starts to absorb more water at relative humidity levels higher than 77%. Analogous results for sorption isotherms of PGM and BSM have been observed at 25 and 50 °C (data not shown). For example, at 50 °C, the sorption isotherm of PGM shows higher water sorption capacity than BSM at RH levels lower than 79% (Supporting Information). It is expected that the energy of interaction of water with charged polymers should be stronger than with noncharged polymers. For example, since BSM is more charged[51−53] than PGM (see

dx.doi.org/10.1021/jp212495t | J. Phys. Chem. B 2012, 116, 5047−5055

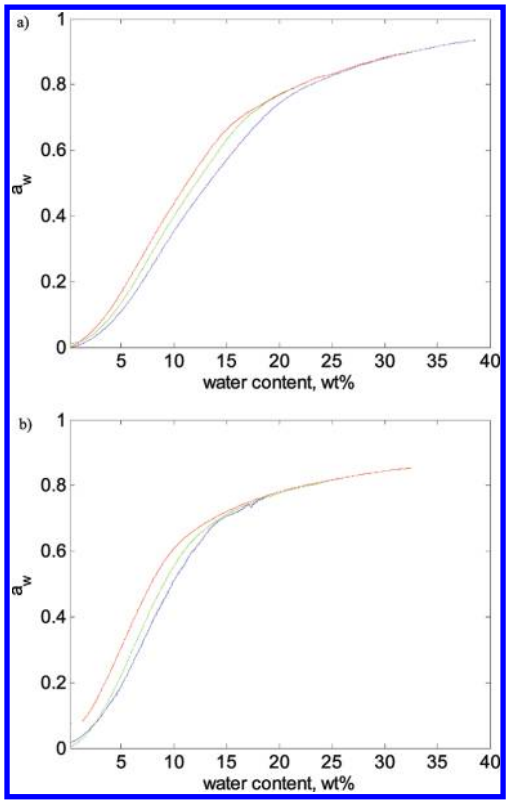

Figure 3. Sorption isotherms of PGM (a) and BSM (b) at different temperatures: 25 (blue line), 40 (green line), and 50 (red line) °C.

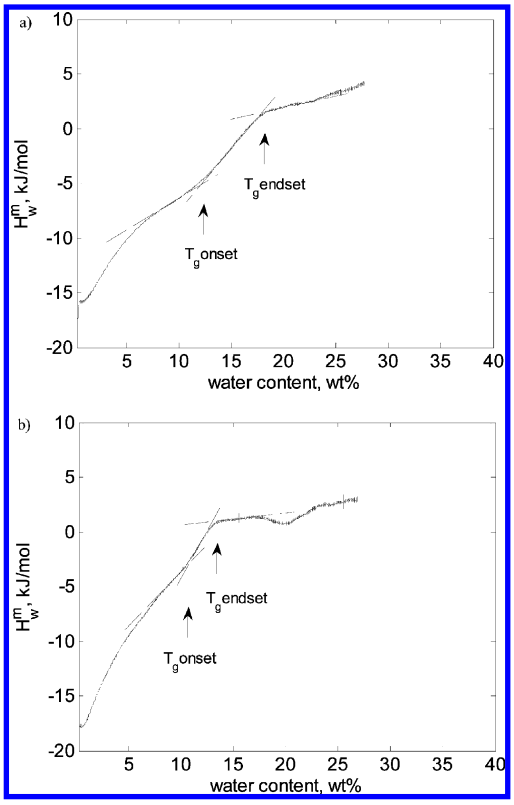

Figure 4. Enthalpy of hydration of PGM (a) and BSM (b) at T = 40 °C. Glass transition corresponds to the step on the curves. Dashed lines demonstrate the glassy and elastic state of mucin in the glass transition region. Arrows show the onset and the endset of the glass transition.

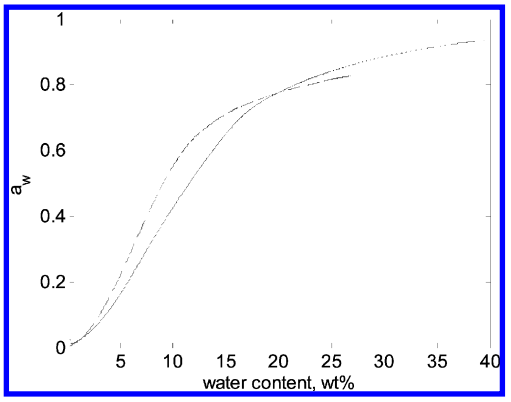

Figure 5. Sorption isotherms of PGM (solid line) and BSM (dashed line) at 40 °C.

below), the enthalpy of hydration of BSM is expected to be more exothermic. However, the enthalpy of hydration of PGM and BSM (Figure 4) has an exothermic and approximately same value at zero water content. Hence, the presence of more charged groups in BSM molecule does not affect the energy of hydration. The same effect was observed in a calorimetric study of hydration of charged and noncharged carbohydrates at low water contents.[36] This effect was explained by the *ab initio* quantum mechanics calculations of interactions of ionic groups presented in charged carbohydrate polymers.[36] *Ab initio* calculations show that the interaction energy[36] between sugar rings and ionic groups is stronger than between water and ionic groups. Then, carbohydrates can solvate ionic groups even more effectively than water molecules do. The enthalpy of hydration of PGM and BSM (Figure 4) has an exothermic effect in the beginning of the sorption process because the mucin system is in the glassy state but not because of strong water−ion interactions. Therefore, electrostatic interactions cannot explain the difference in hydrophilicity between PGM and BSM at low RH levels. The difference in sorption capacity at low water contents between mucins from two different animal sources can be explained by the difference in carbohydrate/protein content in PGM[52,53] and BSM.[31,51,53−55] The water sorption capacity of biopolymers is determined by the number of available sorption sites. At low humidity levels, the water sorption by proteins occurs mostly at carbohydrate side chains, while most of the globular protein part is not available for water sorption. For instance, comparing sorption isotherms of lysozyme[34] and xanthan gum,[36] one can see that at the same relative humidity level, 30%, the mass of absorbed water for xanthan gum is 10 wt %, which is higher than the mass of absorbed water for lysozyme, 5 wt %. Hence, during the initial water sorption process, water molecules primarily and easily interact with carbohydrate side chains in mucin. For example, the content of carbohydrates in PGM is about 83−86 wt %[52,53] and in BSM is around 61−69 wt %.[31,51,53−55] This indicates that PGM contains a higher amount of carbohydrates than BSM. In accordance with this, in the beginning of the water sorption process, more water is absorbed by PGM, and therefore, PGM has a higher sorption capacity at low RH level (Figure 5). Indeed, on the basis of literature data, carbohydrates absorb more water than proteins. However, at high relative humidity level, higher than 77%, BSM starts to absorb more water than PGM possibly due to electrostatic repulsive forces between carbohydrate side chains in BSM. As it is known from the literature, the electrostatic

dx.doi.org/10.1021/jp212495t | J. Phys. Chem. B 2012, 116, 5047−5055

properties of mucins are determined by carbohydrate side chains[46,56] which are often negatively charged due to the presence of sialic acid residue and sulfate groups. A negative charge on the mucin molecule is created by the sialic acid regions which attract polar molecules of water. Since the content of sialic acid in both types of mucin is different, the electrostatic repulsive forces in mucins differ as well. For example, the sialic acid content in PGM is about 2−3 wt %.[51−53] Therefore, PGM is considered as a weakly charged molecule.[46] BSM consists of a much higher amount of sialic acid which is about 32−36 wt %.[51−53] Consequently, the electrostatic repulsive forces are stronger in BSM than in PGM, and the sorption capacity of BSM is higher at relative humidity higher than 77% (Figure 5).

The sorption isotherms of PGM and PGMC at 40 °C are presented in Figure 6. It is shown that PGMC absorbs less

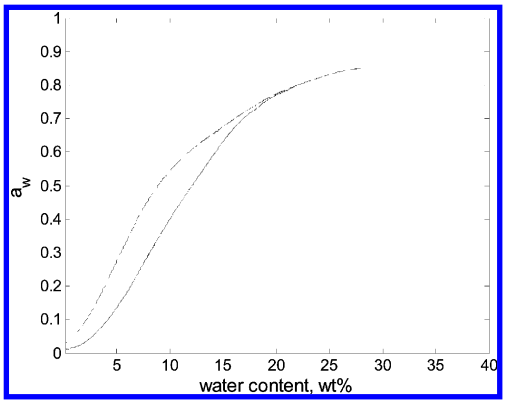

Figure 6. Sorption isotherms of PGM (solid line) and PGMC (dashed line) at 40 °C.

water than commercial PGM from Sigma at low relative humidities. Indeed, experimental PGMC has not been purified. According to the literature data, it consists not only of water and mucin but also of enzymes, proteins, electrolytes, and lipids.[5,13−16] Those impurities could be a reason of absorbing less water at low RH. Sorption isotherms converge at higher RH levels when the glass transition occurs (see below).

The method of sorption calorimetry also allows studying the glass transition of biomolecules at a constant temperature.[33−36] For instance, measuring the enthalpy of mixing of water at the same time with the water sorption of mucin can describe the properties of the water−mucin system. As an example, the partial molar enthalpy of mixing of water as a function of water content at 40 °C for both BSM and PGM is presented in Figure 4. Figure 4 shows that the values of the partial molar enthalpy of mixing of water for both mucin systems are exothermic in the beginning of sorption and become endothermic in the end of the hydration process. Thus, changes in H_w^m from negative to positive values reflect the glass-to-elastic transition in water−mucin systems. The value of H_w^m at zero water content at 40 °C for PGM is −16 kJ/mol and for BSM is −17 kJ/mol. The values of the enthalpy of hydration at zero water content at 25 and 50 °C are also exothermic (Supporting Information). From the literature data on sorption calorimetry, it is known that such exothermic values of H_w^m are typical for the hydration process of proteins and polymer systems.[33,34,36,57] For instance, typical values of H_w^m for lysozyme systems at 25 °C have been observed as −20 kJ/mol;[32] for xanthan gum[36] and for microcrystalline cellulose, it is about −19 kJ/mol.[57]

According to Figure 4, the glass transitions of PGM (a) and BSM (b) take place at water contents for PGM ∼ 15 wt % and for BSM ∼ 12 wt %. They occur approximately at the same RH levels for both types of mucin. Figure 7 shows the dependence

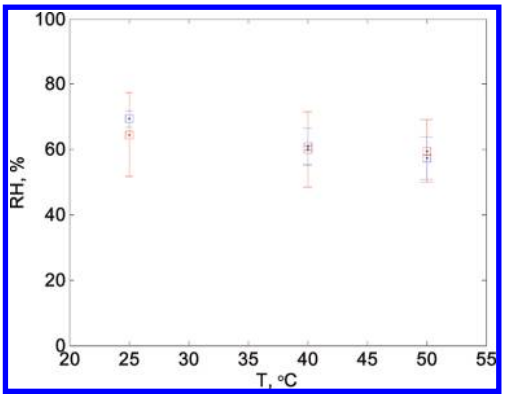

Figure 7. RH levels in PGM (red) and BSM (blue) at the midpoints of the glass transition (squares). The error bars show the onset and the endset of the glass transition.

of relative humidity on the temperature at which glass transition occurs. It demonstrates the weak dependence and the relative humidity levels at which the glass transition of PGM and BSM occurs are between 60 and 70% (Figure 7). Thus, "in vitro" glass transition occurs at high RH levels, between 60 and 70%. However, "in vivo", the values of humidity at which Tg is happening are lower. For example, "in vivo" below 30% RH, the eyes and skin become dry and below 10% RH the nasal mucous membrane becomes dry as well as skin and eyes.[7] That difference between values of RH "in vitro" and "in vivo" shows the presence of a water activity gradient. For instance, because the water is supplied from the internal body, the eyes, skin, and nasal mucous do not dry out immediately when they in contact with a dry atmosphere.

Using sorption and differential calorimetric data, the phase diagram of PGM (Figure 8) was constructed. The phase diagram reflects the glass transition as a function of temperature and hydration levels. A detailed explanation of the phase

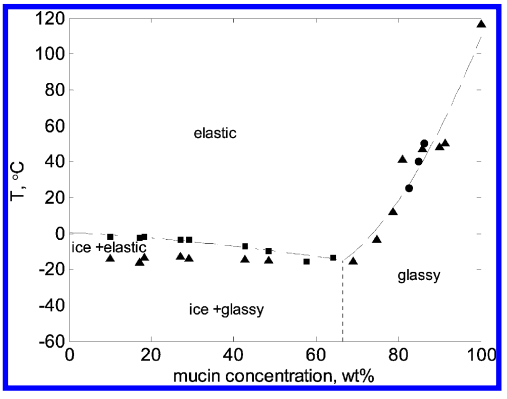

Figure 8. Phase diagram of PGM using sorption calorimetric (circles) and DSC (triangles, squares) data. There are two regions of different Tg: dependent and independent of hydration levels. In particular, at mucin concentrations from 0 to 67 wt %, the glass transition occurs at the same temperature, around −15 °C. At higher concentrations of mucin, Tg is increasing with increasing mucin concentrations.

dx.doi.org/10.1021/jp212495t | J. Phys. Chem. B 2012, 116, 5047−5055

diagram is presented in the following part describing the DSC data.

DSC. Samples of PGM with different water contents have been studied by DSC. Scans of the samples with low mucin concentrations are different from the scans of the mixtures with higher mucin concentrations. As a result, it has been reflected on the phase diagram of PGM (Figure 8). According to the phase diagram, there are two regions of different Tg: dependent and independent of hydration levels. For example, at mucin concentrations from 0 to 67 wt %, the glass transition occurs at the same temperature, around −15 °C. At higher concentrations of mucin, Tg is increasing with increasing mucin concentrations. As an example, scans with low and high mucin content are presented in Figure 9. Thermograms are presented

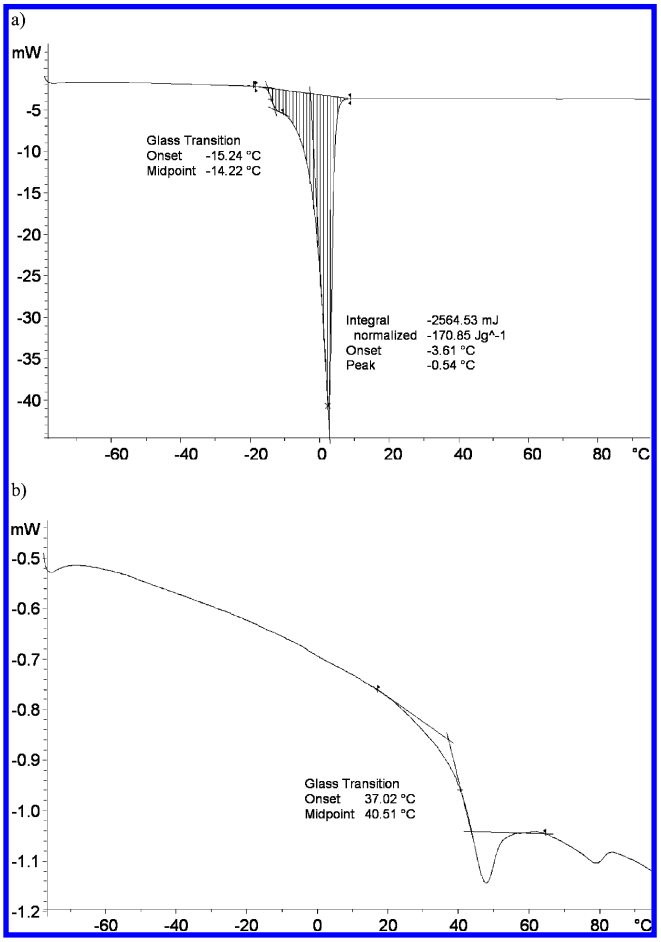

Figure 9. DSC scan of (a) 29.14 wt % PGM and (b) 80.91 wt % PGM. Glass transition is shown with dashed lines.

as a result of subtracting a blank scan with empty pan from each scan with studied system. A scan with low mucin content (29 wt %) (Figure 9a) shows two endothermic processes: a step corresponding to the independent of hydration levels glass transition and a peak representing ice melting. Figure 9b presents a scan with high mucin content (81 wt %), where the endothermic step, representing the dependent on hydration levels glass transition, is obtained. Moreover, the values of the difference in heat capacity (ΔC_p) for independent and dependent on hydration levels Tg are different. For instance, $\Delta C_{p(29wt\%)}$ is 1.937 J/g·K and $\Delta C_{p(81wt\%)}$ is 0.347 J/g·K. Higher ΔC_p at low mucin concentrations is explained by the presence of a two-phase area in the system (Figure 8). ΔC_p of that process includes ΔC_p of the independent mucin glass transition and ΔC_p of the ice melting. However, at high mucin concentrations, ΔC_p is lower because only one phase region is present, where the dependent glass transition of the mucin is observed.

Using DSC data, obtained for mucin samples with high water contents, and the literature enthalpy of fusion of water,[58,59] the mass of nonfreezing water per gram of PGM (protein-bound water[58,60]) was calculated (Figure 10). The average amount of

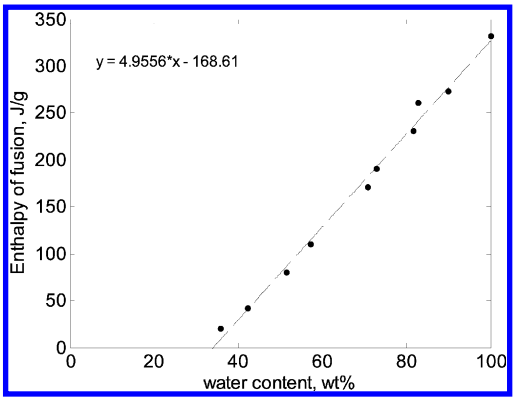

Figure 10. The mass of nonfreezing water per gram of PGM, calculated using DSC data. At ΔH_{fusion} = 0 J/g: water content = 34 wt % and PGM content = 66 wt %. Amount of nonfreezing water: 34/66 = 0.51 g/g of mucin.

nonfreezing water is about 0.51 g/g of mucin. For example, to compare with lysozyme, it is about 0.34 g/g of lysozyme.[60]

The glass transition temperatures, obtained in sorption calorimetry and DSC, as a function of mucin concentration are shown in Figure 8. Data obtained by both calorimetric methods are in good agreement. The dashed lines are drawn as a guide for the eye to follow the glass transition line. As it was mentioned above, the phase diagram shows that there are regions with two different types of glass transitions: dependent and independent of hydration levels. On the phase diagram, independent Tg is shown up to 67 wt % mucin. Below that Tg, there is a two-solid-phase area: ice and mucin in a glassy state. After glass transition, two phases are present: ice and mucin in elastic state. With increasing mucin content (up to 67 wt %), the onset of ice melting is decreasing, as shown on the phase diagram with a blue dashed line. Further increase of temperature and mucin content leads to one phase region: mucin in elastic state. Samples with mucin concentrations above 67 wt % have the Tg dependent on the water content. The glass transition temperature is decreasing with increasing water content. The decrease of Tg is a result of water plasticization.[61] It is known that increasing water content of a system results in plasticization of the amorphous solids and hence in reducing Tg.[62] Below the dependent Tg, one solid phase of the system is observed, and it is mucin in glassy state. The intersection of dependent and independent Tg curves on Figure 8 is considered as the concentration of mucin in a glassy state in the solid phase area. The water content decreases and the onset of ice melting slightly reduces, but the mucin concentration is not changing. Therefore, samples with mucin concentrations up to 67 wt % show independent and constant Tg. For instance, Singh and Roos[62] have reported the same indication of dependent and independent glass transition temperatures for mixed sugar−polymer systems. The results

dx.doi.org/10.1021/jp212495t | J. Phys. Chem. B 2012, 116, 5047−5055

in Figure 8 obtained by sorption calorimetry and DSC are not in agreement with data presented by Davies and Viney[3] who suggested that the glass transition in PGM from Sigma takes place at ~25 °C and is independent of the concentration. According to results on the phase diagram (Figure 8), Tg of PGM is isothermal at high water contents and is dependent on the temperature and on the water content at low hydration levels.

CONCLUSIONS

In this work, we investigated the effect of hydration on the structural and thermodynamic properties of mucin using AFM, DSC, and sorption calorimetry. The results from this study show that:

- AFM indicates the presence of a dumbbell structure as well as a fiber-like structure in PGM samples. The experimental volume of the dry dumbbell structure obtained by AFM is 3140 ± 340 nm^3. In the case of BSM samples, only fiber-like structures were observed in AFM experiments.
- The sorption isotherm of PGM shows that up to 78% relative humidity PGM absorbs more water than BSM. BSM absorbs more water at relative humidity levels higher than 78%.
- The value of the partial molar enthalpy of mixing of water at zero water content at 25 °C for mucin is about −20 kJ/mol. Such exothermic values of H_w^m are typical for the hydration process of proteins and polymer systems.
- The glass transitions of PGM and BSM occur at relative humidity levels between 60 and 70%. The RH at which Tg occurs is weakly dependent on the temperature and type of mucin.
- The phase diagram reflects two regions of different Tg: dependent and independent of hydration levels. At mucin concentrations from 0 to 67 wt %, the glass transition occurs at the same temperature, around −15 °C. At higher concentrations of mucin, Tg is increasing with increasing mucin concentrations.
- The mass of nonfreezing water is 0.51 g/g of PGM which is higher than the mass of nonfreezing water of globular proteins due to the carbohydrate content in mucin molecule.

ASSOCIATED CONTENT

Supporting Information

Comparison of sorption isotherms of PGM and BSM at 50 °C and enthalpy of hydration of PGM and BSM at 25 and 50 °C. This material is available free of charge via the Internet at http://pubs.acs.org.

AUTHOR INFORMATION

Corresponding Author

*Address: Faculty of Health and Society, Malmö University, SE-205 06 Malmö, Sweden. E-mail: Yana.Znamenskaya@mah.se.

Notes

The authors declare no competing financial interest.

ACKNOWLEDGMENTS

Financial support from Malmo University, the Knowledge Foundation (KK-stiftelsen), and the Gustav Th Ohlsson Foundation is gratefully acknowledged. We would like to thank Julia Davies for discussions and helping to extract PGMC from the pig stomach.

REFERENCES

(1) Allen, A. *Trends Biochem. Sci.* **1983**, *8*, 169−173.
(2) Thornton, D. J.; Rousseau, K.; McGuckin, M. A. *Annu. Rev. Physiol.* **2008**, *70*, 459−486.
(3) Davies, J. M.; Viney, C. *Thermochim. Acta* **1998**, *315*, 39−49.
(4) Perez-Vilar, J.; Hill, R. L. *J. Biol. Chem.* **1999**, *274*, 31751−31754.
(5) Bansil, R.; Turner, B. S. *Curr. Opin. Colloid Interface Sci.* **2006**, *11*, 164−170.
(6) Lincoln, B. J.; Simpson, T. R. E.; Keddie, J. L. *Colloids Surf., B* **2004**, *33*, 251−258.
(7) Sunwoo, Y.; Chou, C.; Takeshita, J.; Murakami, M.; Tochihara, Y. *J. Physiol. Anthropol.* **2006**, *25*, 229−238.
(8) Ratjen, F. A. *Respir. Care* **2009**, *54*, 595−602.
(9) Oliver, A.; Canton, R.; Campo, P.; Baquero, F.; Blazquez, J. *Science* **2000**, *288*, 1251−1253.
(10) Bae, H.; Li, Y.-H.; Na, Y.; Jung, Y.; Lee, S.; Yang, J.; Kim, D. *Genes Genomics* **2010**, *32*, 429−435.
(11) Amft, N.; Bowman, S. J. *Scand. J. Immunol.* **2001**, *54*, 62−69.
(12) Sarin, S.; Undem, B.; Sanico, A.; Togias, A. *J. Allergy Clin. Immunol.* **2006**, *118*, 999−1014.
(13) Creeth, J. M. *Br. Med. Bull.* **1978**, *34*, 17−24.
(14) Harding, S. E. The Macrostructure of Mucus Glycoproteins in Solution. *Advances in Carbohydrate Chemistry and Biochemistry*; Tipson, R. S., Derek, H., Eds.; Academic Press: San Diego, 1989; Vol. *47*, pp 345−381.
(15) Peppas, N. A.; Buri, P. A. *J. Controlled Release* **1985**, *2*, 257−275.
(16) Patel, M. M.; Smart, J. D.; Nevell, T. G.; Ewen, R. J.; Eaton, P. J.; Tsibouklis, J. *Biomacromolecules* **2003**, *4*, 1184−1190.
(17) Celli, J. P.; Turner, B. S.; Afdhal, N. H.; Ewoldt, R. H.; McKinley, G. H.; Bansil, R.; Erramilli, S. *Biomacromolecules* **2007**, *8*, 1580−1586.
(18) Svensson, O.; Arnebrant, T. *Curr. Opin. Colloid Interface Sci.* **2010**, *15*, 395−405.
(19) Royle, L.; Matthews, E.; Corfield, A.; Berry, M.; Rudd, P.; Dwek, R.; Carrington, S. *Glycoconjugate J.* **2008**, *25*, 763−773.
(20) Parry, S.; Sutton-Smith, M.; Heal, P.; Leir, S. H.; Palmai-Pallag, T.; Morris, H. R.; Hollingsworth, M. A.; Dell, A.; Harris, A. *Biochim. Biophys. Acta* **2005**, *1722*, 77−83.
(21) McColl, J.; Yakubov, G. E.; Ramsden, J. J. *Langmuir* **2007**, *23*, 7096−7100.
(22) Gendler, S. J.; Spicer, A. P. *Annu. Rev. Physiol.* **1995**, *57*, 607−634.
(23) MacAdam, A. *Adv. Drug Delivery Rev.* **1993**, *11*, 201−220.
(24) Di Cola, E.; Yakubov, G. E.; Waigh, T. A. *Biomacromolecules* **2008**, *9*, 3216−3222.
(25) Yakubov, G. E.; Papagiannopoulos, A.; Rat, E.; Easton, R. L.; Waigh, T. A. *Biomacromolecules* **2007**, *8*, 3467−3477.
(26) Momoh, M. A.; Adikwu, M. U.; Ibezim, C. E.; Ofokansi, K. C.; Attama, A. A. *Asian Pac. J. Trop. Med.* **2010**, *3*, 458−460.
(27) Viney, C.; Huber, A. E.; Verdugo, P. *Macromolecules* **1993**, *26*, 852−855.
(28) Viney, C. *Biorheology* **1999**, *36*, 319−323.
(29) Waigh, T. A.; Papagiannopoulos, A.; Voice, A.; Bansil, R.; Unwin, A. P.; Dewhurst, C. D.; Turner, B.; Afdhal, N. *Langmuir* **2002**, *18*, 7188−7195.
(30) Builders, P. F.; Kunle, O. O.; Adikwu, M. U. *Int. J. Pharm.* **2008**, *356*, 174−180.
(31) Bettelheim, F. A.; Block, A. *Biochim. Biophys. Acta* **1968**, *165*, 405−409.
(32) Kocherbitov, V.; Arnebrant, T. *Langmuir* **2010**, *26*, 3918−3922.
(33) Kocherbitov, V.; Arnebrant, T. *J. Phys. Chem. B* **2006**, *110*, 10144−10150.
(34) Kocherbitov, V.; Arnebrant, T.; Soderman, O. *J. Phys. Chem. B* **2004**, *108*, 19036−19042.
(35) Kocherbitov, V.; Soderman, O. *Langmuir* **2004**, *20*, 3056−3061.

(36) Kocherbitov, V.; Ulvenlund, S.; Briggner, L. E.; Kober, M.; Arnebrant, T. *Carbohydr. Polym.* **2010**, *82*, 284−290.
(37) Wadso, L.; Markova, N. *Rev. Sci. Instrum.* **2002**, *73*, 2743−2754.
(38) Greenspan, L. *J. Res. Natl. Bur. Stand., Sect. A* **1977**, *81*, 89−96.
(39) Horcas, I.; Fernandez, R.; Gomez-Rodriguez, J. M.; Colchero, J.; Gomez-Herrero, J.; Baro, A. M. *Rev. Sci. Instrum.* **2007**, 78.
(40) Wadso, I.; Wadso, L. *Thermochim. Acta* **1996**, *271*, 179−187.
(41) Kocherbitov, V. *Thermochim. Acta* **2004**, *414*, 43−45.
(42) Hong, Z. N.; Chasan, B.; Bansil, R.; Turner, B. S.; Bhaskar, K. R.; Afdhal, N. H. *Biomacromolecules* **2005**, *6*, 3458−3466.
(43) Deacon, M. P.; McGurk, S.; Roberts, C. J.; Williams, P. M.; Tendler, S. J. B.; Davies, M. C.; Davis, S. S.; Harding, S. E. *Biochem. J.* **2000**, *348*, 557−563.
(44) McMaster, T. J.; Berry, M.; Corfield, A. P.; Miles, M. J. *Biophys. J.* **1999**, *77*, 533−541.
(45) Brunelli, R.; Papi, M.; Arcovito, G.; Bompiani, A.; Castagnola, M.; Parasassi, T.; Sampaolese, B.; Vincenzoni, F.; De Spirito, M. *FASEB J.* **2007**, *21*, 3872−3876.
(46) Yakubov, G. E.; Papagiannopoulos, A.; Rat, E.; Waigh, T. A. *Biomacromolecules* **2007**, *8*, 3791−3799.
(47) Ho, S. B.; Shekels, L. L.; Toribara, N. W.; Kim, Y. S.; Lyftogt, C.; Cherwitz, D. L.; Niehans, G. A. *Cancer Res.* **1995**, *55*, 2681−2690.
(48) Nordman, H.; Davies, J. R.; Carlstedt, I. *Biochem. J.* **1998**, *331*, 687−694.
(49) Reis, C. A.; David, L.; Correa, P.; Carneiro, F.; de Bolos, C.; Garcia, E.; Mandel, U.; Clausen, H.; Sobrinho-Simoes, M. *Cancer Res.* **1999**, *59*, 1003−1007.
(50) Nordman, H.; Davies, J. R.; Lindell, G.; de Bolos, C.; Real, F.; Carlstedt, I. *Biochem. J.* **2002**, *364*, 191−200.
(51) Bhavanandan, V. P.; Hegarty, J. D. *J. Biol. Chem.* **1987**, *262*, 5913−5917.
(52) Scawen, M.; Allen, A. *Biochem. J.* **1977**, *163*, 363−368.
(53) Sandberg, T.; Blom, H.; Caldwell, K. D. *J. Biomed. Mater. Res., Part A* **2009**, *91A*, 762−772.
(54) Bettelheim, F. A.; Dey, S. K. *Arch. Biochem. Biophys.* **1965**, *109*, 259−265.
(55) Tettamanti, G.; Pigman, W. *Arch. Biochem. Biophys.* **1968**, *124*, 41−50.
(56) Lee, S.; Muller, M.; Rezwan, K.; Spencer, N. D. *Langmuir* **2005**, *21*, 8344−8353.
(57) Kocherbitov, V.; Ulvenlund, S.; Kober, M.; Jarring, K.; Arnebrant, T. *J. Phys. Chem. B* **2008**, *112*, 3728−3734.
(58) Rahman, M. S.; Al-Saidi, G.; Guizani, N.; Abdullah, A. *Thermochim. Acta* **2010**, *509*, 111−119.
(59) Haida, O.; Matsuo, T.; Suga, H.; Seki, S. *J. Chem. Thermodyn.* **1974**, *6*, 815−825.
(60) Miyazaki, Y.; Matsuo, T.; Suga, H. *J. Phys. Chem. B* **2000**, *104*, 8044−8052.
(61) Roos, Y. H.; Karel, M. *Biotechnol. Prog.* **1990**, *6*, 159−163.
(62) Singh, K. J.; Roos, Y. H. *Int. J. Food Prop.* **2010**, *13*, 184−197.